Polymer Bulletin 52, 297-305 (2004)
DOI 10.1007/s00289-004-0288-7

Polymer Bulletin

Combustion resistant nanocomposites from water/AOT/MMA reverse microemulsions

Liehui Ge and John Texter (✉)

College of Technology, Eastern Michigan University, Ypsilanti, MI 48197
jtexter@emich.edu

Received: 16 April 2004/Revised version: 23 July 2004/Accepted: 26 July 2004

Summary

A reverse microemulsion domain in the ternary water, AOT, and MMA (methyl methacrylate) system is reported at 22±1°C and compositions in this domain are polymerized at 70°C to produce nanocomposites of surfactant and water in PMMA. While limited microphase separation occurs during polymerization the resulting solids are translucent and no macroscopic phase separation occurs. Optical and thermal analysis indicates that the water is distributed uniformly throughout the nanocomposite and is mostly tightly bound to the surfactant headgroup and cannot freeze. The small amount of incorporated water that is freezable resides in pores or droplets about 12 nm or less in diameter. The translucency can be assigned to some sort of very limited microphase separation of the surfactant that occurs during polymerization. Ignition and TGA analyses indicate that the combustion resistance is mostly due to the incorporated AOT.

Introduction

A variety of nanocomposites can be derived from microemulsions by polymerizing monomers in either the aqueous or oil domains or in both domains [1-5]. More recently nanoparticles are being synthesized in reverse microemulsion systems [6-8], wherein the oil phase is a reactive monomer, and then microemulsion polymerization is used to transform the nanosuspension into a solid nanocomposite.

We are interested in developing methods to adjust microemulsion microstructure so that nanocomposites may be obtained that remain transparent after polymerization and have controlled nanoporosity. Aerosol OT (AOT; bis[2-ethylhexyl] sulfosuccinate, sodium salt) is very effective for producing water in oil reverse microemulsions [9,10]. Quite large L_2 domains are often obtained. As our initial "oil" we use the monomer methylmethacrylate (MMA), since this monomer is readily polymerized by radical chain polymerization with thermal initiation.

Microemulsions

A partial ternary phase diagram at room temperature (22±1°C) is illustrated in Fig. 1. A large L_2 domain is obtained. An L_1 domain was also mapped, but it is rather small on the scale of Fig. 1 and it will be reported in a full paper subsequently. A somewhat

different phase diagram for this system is presented in Pavel's thesis [7]; our measurements agree with her's for MMA/water ratios greater than 1.5. At about equal weight AOT and MMA (see the dotted tie-line in Fig. 1), the solubilized water increases markedly (nearly doubles) as the AOT/MMA ratio is increased. The entire L_2 domain has not been mapped. We did not investigate the boundary to this region above a 75/25 AOT/MMA weight ratio, so the upper bound to this domain is approximated by the medium dashed line running nearly parallel with the water-AOT axis. A short segment of five dashes is shown along the 30/70 AOT/MMA tie-line between the AOT-MMA axis and the L_2 domain boundary. This segment is a locus of microemulsion polymerization.

Polymerizations

AIBN (azoisobutyronitrile; Aldrich) was used as thermal initiator. It was used at 0.1 and 1% of total monomer and was dissolved in the MMA. Reverse microemulsions for polymerization were formulated having 70/30 AOT/MMA weight ratio. These microemulsions were made with no water and with 5 and 10% w/w added water. They were then placed in culture tubes or in 5 mm inner diameter NMR tubes for polymerization. These tubes were then immersed in an oil bath at 70°C. After 4-6 hours the solid rods were removed from the tubes (by breaking the tubes). Since microemulsions are in fact single phase solutions (with nanoscale heterogeneity

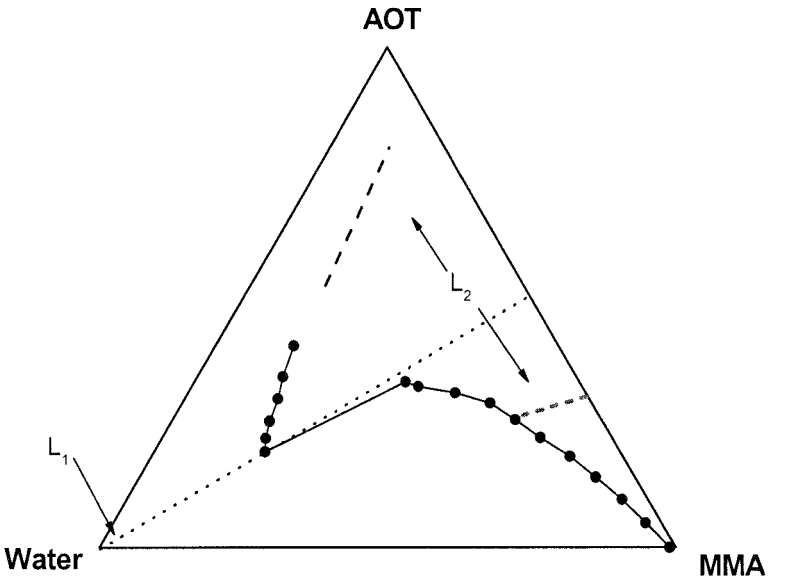

Figure 1. Partial ternary phase diagram of the water/AOT/MMA system at room temperature (22±1°C). Axes have units of weight fraction. The three-dash line running along the 30/70 AOT/MMA tie-line within the L_2 domain marks the locus along which we effected thermally initiated polymerization. The highest compositions verified as belonging to the L_2 domain were found along the 75/25 AOT/MMA tie-line, so the undetermined upper boundary is approximated by the dashed line running almost parallel to the water-AOT axis. The L_1 domain is too small to resolve at this scale.

formed by complex surfactant aggregates), polymerization of reverse microemulsions wherein the pseudo-continuous monomer phase is polymerized constitutes a special case of bulk polymerization.

The rods so obtained from the NMR tubes for these compositions are illustrated in Fig. 2 along with a PMMA (polymethylmethacrylate) control. The photography was done so as to highlight the translucent opacity obtained for the microemulsion samples and the marked clarity obtained for the PMMA control. As can be seen in the rods with AOT pictured in Fig. 2, the optical densities of the rods were not constant. The microphase separation that did occur, therefore, was not completely uniform. The turbidity or opacity in the water-containing samples is somewhat greater, however, than that of the AOT sample without added water. The detailed nature of this

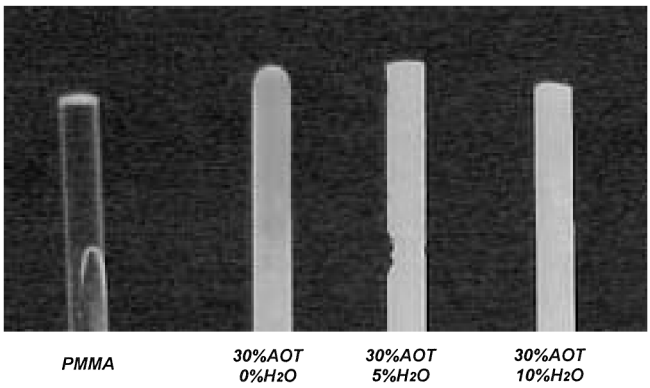

Figure 2. Photograph of the control (PMMA) and AOT/PMMA (30/70 AOT/MMA with 0, 5, and 10% w/w added water) samples obtained by polymerizing solution or microemulsions, respectively, in NMR tubes with 1% initiator.

microphase separation will have to await further investigation. Since translucent opacity was obtained in the sample without added water, some of the microphase separation can be unequivocally assigned as AOT microphase separation. A somewhat related phenomenon was reported by Pavel and Mackay [6] in a study of water/MMA microemulsions formulated with a polymerizable surfactant. They found that after polymerization, aggregates exhibiting very slight turbidity could be assigned as polyelectrolytes derived from the polymerizable surfactant and were identified in micrographs obtained by TEM.

Characterization

The samples made with different levels of AIBN (0.1 or 1.0% relative to total monomer) were analyzed for polystyrene-equivalent molecular weight by examining dilute samples (0.1% w/w)) in THF by size exclusion chromatography using an HP 1050 series HPLC with an HP 1047A RI detector and three Phenogel columns in series for a molecular weight range of 500 to 1,000,000. Number-average (M_n), weight-average (M_w), and z-average (M_z) molecular weight results and the polydispersity index (PI) are summarized in Table 1. The level of initiator, AIBN, appears to have the greatest effect. The ten-fold increase in AIBN concentration

Table 1. Molecular weight analysis of PMMA produced by microemulsion polymerization of 30:70 AOT:MMA microemulsions containing 0-10% w/w water.

Sample	log M_n	log M_w	log M_z	PI
0.1% AIBN				
AOT/PMMA 0% water	5.79	6.31	6.53	3.33
AOT/PMMA 5% water	5.73	6.32	6.55	3.88
AOT/PMMA 10%water	5.78	6.32	6.54	3.49
1.0% AIBN				
PMMA control	5.16	5.73	6.12	3.65
AOT/PMMA 0% water	5.19	5.86	6.19	4.65
AOT/PMMA 5% water	5.06	5.75	6.10	4.81
AOT/PMMA 10% water	5.14	5.84	6.17	4.99

resulted in an approximately 70% drop in M_w (a little more for M_n and a little less for M_z). Similarly, the polydispersity index increased by about 33% with increasing AIBN. It appears that the main effect of the surfactant and microemulsion polymerization on the resulting moments of the molecular weight distribution is on the polydispersity, as the moments appear to be, within experimental uncertainties, indistinguishable from the PMMA control values. For the samples with 1% AIBN initiation, the polydispersity is about 30% greater than for the PMMA control. While it is not apparent from the moments listed in Table 1, the PMMA control exhibited a bimodal distribution of dw/dlogM plotted as a function of logM, with a peak at about 5.3 in logM and a significant shoulder (85% of peak) just below a logM of 6. All of the microemulsion polymerization samples also exhibited bimodal plots, but in the case of 1% AIBN initiation the peak was found just a little above (~0.15) the logM_w values with a lower shoulder (logM of 4.7-4.8, ~35% of peak). These differences are illustrated in Fig. 3 where the differential weight-average molecular weight distributions are illustrated for the PMMA control and for the AOT/PMMA 0% water and AOT/PMMA 10% water samples. The AOT appears to promote formation of higher weight-average molecular weights.

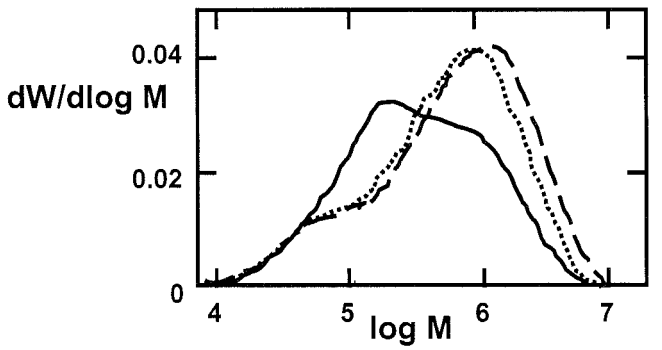

Figure 3. Differential weight-average molecular weight distributions for a PMMA control (solid line) and for PMMA synthesized in AOT/MMA reverse microemulsions with 0% water (dotted line) and with 10% water (dashed line); AIBN used for initiation at 1% (w/w) of monomer.

The samples illustrated in Fig. 2 were also examined by DSC. Interestingly, the sample containing 5% water did not have any freezable water, so all of the water in sample 2 must of necessity be water of hydration of the surfactant headgroup (sodium ion, sulfonate group, ester groups). Since it is generally accepted that 5-8 water molecules hydrate AOT in reverse micelles and microemulsions [11], the mole ratio of water to AOT is only 4.3 in the 5% water sample. Freezable water was identified in the 10% water sample. The freezing point of this water was depressed to -11.5°C or lower. If we assume this freezing had the same heat of fusion as bulk water, the amount of freezable water corresponded to about 10% of the sample's water or about 1% overall. This suggests in this system, therefore, that about 9% of the water is unfreezable, and this level corresponds to a water/AOT mole ratio of about 8.3.

Glass transition temperatures were also measured for the PMMA control samples and for the AOT samples that did not contain any water. The control PMMA initiated with 0.1% AIBN had a T_g of 105°C, while the control initiated with 1% AIBN had a lower T_g at 103°C. The AOT/PMMA samples without added water and initiated with 0.1 and 1.0 % AIBN yielded T_g values of 93°C and 100°C, respectively. The T_g values in both the control PMMA and the AOT/PPMA samples increase with increasing initiator (and lower molecular weight). At the same initiator level (with respect to total monomer), the AOT/PMMA samples have lower T_g values than the corresponding controls. Thus the incorporated AOT can be ascribed a plasticizing effect. This effect appears to be much more severe at lower initiator.

Pieces of polymer produced in culture tubes were subjected to an ignition test by placing a sample in a Fisher burner at the tip of a blue flame-point to ignite the sample and then removing the sample to see if combustion would be sustained. This test is a modified form of the UL 1581 (VW-1) ignition test that uses a tirrill burner [12]. Preliminary results are illustrated in Fig. 4. The PMMA control ignited immediately

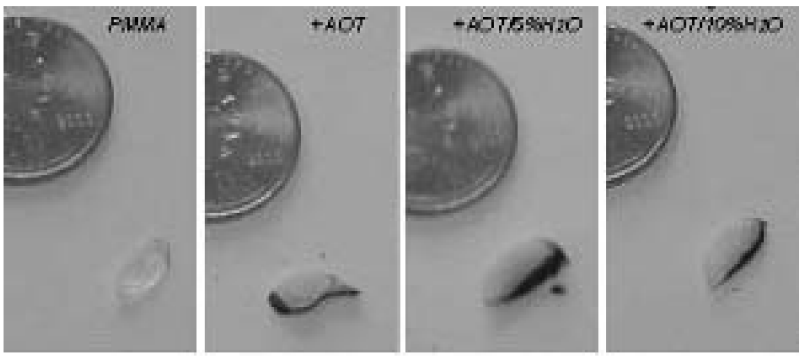

Figure 4. Ignition test results (Fisher burner) obtained for the control (PMMA) and AOT/PMMA (30/70 AOT/MMA with 0, 5, and 10% w/w water) samples such as those illustrated in Fig. 2, but polymerized with 0.1% initiator.

and burned cleanly and continuously until extinguished. The AOT containing samples, after ignition and withdrawal burned more slowly and usually self-extinguished. PMMA is thought to burn cleanly because the heat given off tends to depolymerize the homopolymer, producing gaseous monomer to feed the flame.

PMMA has been considered as a promising solid fuel for space vehicles because of this property [13]. The presence of AOT has a marked effect on the combustion products and temperature, as evidenced by the char illustrated in Fig. 4. AOT itself, when held in the flame as these polymer samples were held, would not ignite. The compound would melt and drop into the burner prior to ignition. We may tentatively conclude that the salt nature of AOT is responsible for most of the combustion resistance of these polymers.

Thermal stability using a thermogravimetric analyzer (TA Instruments Model SDT 2960 simultaneous DTA-TGA) was examined in air over the room temperature to 600°C interval with a 10°C per minute heating rate. Results for the compositions illustrated in Fig. 2 are depicted in Fig. 5. The PMMA control decomposes over the 250-350°C interval. The samples containing AOT all deviate from the control sample above 260°C, and this deviation can be assigned to the presence of AOT throughout the samples.

At lower temperature the differences between the control and AOT samples is particularly interesting, as insight into the nanocomposite nature of these materials is obtained. The AOT sample without added water appears to overlap the control curve for PMMA until it deviates to slower decomposition above about 290°C. The sample containing 5% water does not begin to release water until the temperature has reached about 90°C, and this release is not complete until about 260°C when decomposition of the polymer sets in. This finding along with the above cited DSC results that indicate this sample did not contain any freezable water suggests this water is tightly held as water of hydration of the AOT, and further that this material is not particularly porous as the water appears not to be able to completely escape until the polymer itself is undergoing decomposition. Most of it can diffuse out, however, above 100°C (and above the T_g). The 10% water sample shares some of the characteristics of the 5%

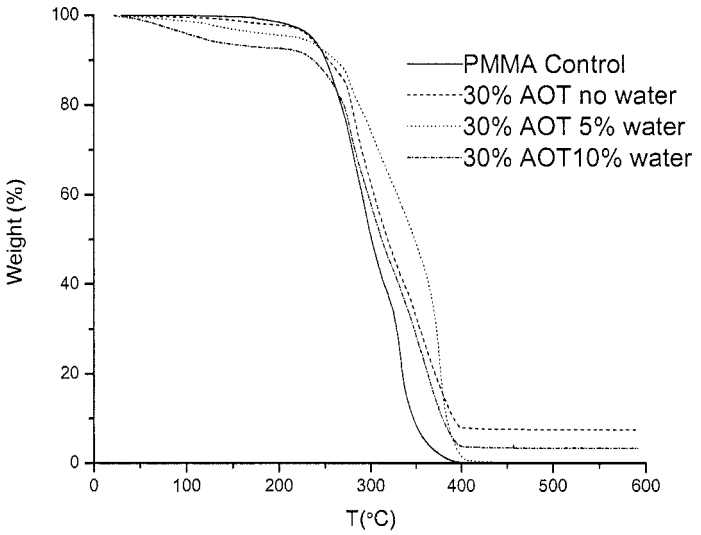

Figure 5. Thermogravimetric analysis of control (PMMA) and AOT/PMMA (30/70 AOT/MMA with 0, 5, and 10% w/w water) samples illustrated in Fig. 2.

sample. While water loss commences just a little bit above room temperature at about 40°C, the overall loss is gradual over the 40-150°C interval and slower still up to 240°C, where polymer decomposition appears to commence. This water loss behavior suggests that the 10% water sample does contain some nanoporosity, but it also appears to hold onto much of its water with the same tenacity as the 5% water sample. The freezing point depression of the freezable water in this sample suggests that the freezable water is in pores or droplets about 12 nm in diameter [14,15]. This pore size is too small to cause any significant light scattering, so we may conclude that all of the translucent turbidity produced in these samples is due to some kind of microphase separation of the surfactant (AOT) during polymerization. There appears to be some nanoporosity, however, since water loss commences at 40°C and continues well below the T_g, above which we expect water transport by diffusion to be enhanced.

The fire resistance imparted by the very fatty AOT is surprising, as we can find no lead in the literature to suggest surfactants in general are fire retardant. A search of over 3 x 10^4 articles describing surfactants revealed only six articles that were associated with fire resistance [16-21]. Two of these references address hydraulic fluids made fire resistant by the incorporation of water in emulsions [16] and in microemulsions [17]; the observed resistance to combustion was assigned to the incorporated water and not to the surfactants used. Two references [18,19] examine the analysis of perfluoronated surfactants and note the use of such surfactants in fire suppressing foam formulations; the perfluoronation is credited with the fire resistant contribution of the surfactants studied, as is the implicitly intumescence for the foams generated. A toxicology report [20] of a foam suppressing surfactant in combination with a fire retardant compound assigned no fire retardancy to the surfactant. Finally surfactants have also been studied in connection with fire resistant cellulose fiber composites [21], but the fire resistance was wholly ascribed to the charring propensity of cotton fibers and to the incorporated ammonium polyphosphate, when compounded with polypropylene. There appear, therefore, to be no teaching in the recent literature that surfactants per se may be useful as fire retardant additives. This phenomenon is perhaps best understood in terms of the implicit salt nature of AOT, as it is a sodium sulfonate [22].

Conclusions

Bulk polymerization can be achieved without inducing macroscopic phase separation of either the incorporated water or the surfactant. The translucent opacity may be assigned to microphase separation of the surfactant. Water incorporated at up to 10% by weight is mostly incorporated uniformly as tightly bound to the surfactant. At 10% w/w water, some of this water is freezable, but highly perturbed relative to bulk water and exhibits a -11.5°C freezing point depression. Nanocomposites containing 5% water appear not to be nanoporous, and the incorporated water is given up only above the T_g. At higher water loading there appears to be some nanoporosity with some water released below the T_g.

Incorporating water as nano- and micro-droplets in bulk polymers might be expected to increase fire resistance. It appears that AOT, an anionic surfactant without any perhalogenation, surprisingly imparts ignition resistance and thermal stability to microcomposites with PMMA.

After this manuscript was submitted, Professor Renate Hiesgen and Dr Jürgen Kraut of the Physics Department at the Fachhochschule in Esslingen examined these and related nanocomposites prepared by microemulsion polymerization by SEM. This examination of the Pt/Pd shadowed fracture surface of a rod AOT/PMMA 0%water sample, such as the one pictured in Fig. 2, revealed a topography exhibiting a very smooth fracture surface pock-marked with hemispherical depressions having an apparently rough surface texture. These hemispherical depressions were of the order of 5-8 microns in diameter. Energy dispersive x-ray elemental analysis showed that the smooth regions were totally devoid of sulfur or sodium, while both of these elements were found in the hemispherical depression regions. The turbidity illustrated in Fig. 2 for this sample and for the samples containing water can therefore be unequivocally ascribed to microphase separation of the AOT during polymerization. This microphase separation into spheroidal domains is most likely into vesicular structures, since AOT is known to favor lamellar mesophase formation [23,24].

Acknowledgements. We wish to thank Professor David Gore for his help with the photography of our sample rods. The molecular weight determinations were kindly provided by Ms. Michelle L. Bruck of Chemir Analytical Services. We also wish to thank Professor Rick Laine of the University of Michigan for allowing us to use his TGA system. We are especially indebted to Professor Renate Hiesgen and Dr. Jürgen Kraut of the Fachhochschule Esslingen for their SEM analyses of these samples.

References

1. Gan LM, Chew CH (1983) J Dispersion Sci Technol 4:291
2. Menger FM, Tsuno T, Hammond GS (1990) J Am Chem Soc 112:1263
3. Kaplin DA, Qutubuddin S (1994) Synth Met 63:187
4. Gan LM, Li T, Chew CH, Teo WK, Gan LH (1995) Langmuir 11:3316
5. Challa V, Kuta K, Lopina S, Cheung HM, von Meerwall E (2003) Langmuir 19:4154
6. Pavel, FM, Mackay, RM (2000) Langmuir 16: 8568
7. Pavel, FM (2001) Thesis, Polymer Blends and Polymer/Nanoparticle Composites from Microemulsions, Clarkson University
8. Xi Q, Zhao CF, Li L, Li L, Zhao L, Cheng SY (2003) Chinese J Chem Phys 16:135
9. Sager WFC (1998) Langmuir 14:6385
10. Li Q, Li T, Wu JG (2002) Colloid Surf A 197: 101
11. Zhou N, Li Q, Wu J, Chen J, Weng S, Xu G (2001) Langmuir 17:4505
12. http://www.kltannehill.com/Technical%20Documents/Cable%20Flame%20Test.htm, downloaded 10 April 2004
13. Fernandez-Pello AC, Rich D, Lautenberger C, Stefanovich A, Metha S, Torero JL, Yuan Z, Ross H, (2003) Piloted ignition of polyproylene/glass composites in forced air flow. In: Sacksteder K (ed) Proceedings of the Seventh International Workshop on Microgravity Combustion and Chemically Reacting Systems, NASA/CP-2003-212376, pp 209-212
14 Ishikiryama K, Todoki M (1995) J Colloid Interface Sci 171: 103
15 Iza M, Woerly S, Danumah C, Kaliaguine S, Bousmina M (2000) Polymer 41: 5885
16 Ratoi M, Spikes HA (1999) Tribology Trans 42:479
17 Regev O, Ezrahi S, Aserin A, Garti N, Wachtel E, Kaler EW, Khan A, Talmon Y (1996) Langmuir 12:668
18 Moody CA, Kwan WC, Martin JW, Muir DCG, Mabury SA (2001) Anal Chem 73:2200
19 Moody CA, Martin JW, Kwan WC, Muir DCG, Mabury SC (2002) Environ Sci Tech 36:545
20 Buscemi DM, Hoffman DJ, Vyas NB, Spann JW, Kuenzel WJ (2002) Arch Environ Contamination Toxicol 43:330

21 Anna P, Zimonyi E, Marton A, Szep A, Matko S, Keszei S, Bertalan G, Marosi G (2003) Macromoleclar Symp 202:245
22 Gilman J (2003) private communication
23 Texter J, Oppenheimer L, Minter JR (1992) Polym Bull 27:487
24 Full AP, Puig JE, Gron LU, Kaler EW, Minter JR, Mourey T, Texter J (1992) Macromolecules, 25:515